ABSTRACT

Title of Thesis: Development of Techniques for Plasma Membrane and Cell Surface Enrichment

Rebecca L. Rose, Master of Science, 2014

Directed By: Catherine Fenselau, Professor, Department of Chemistry and Biochemistry

The goal of this work is to develop and compare two methods of cell surface protein enrichment. The plasma membrane and cell surface proteomes are of great interest for the development of drug targets and increasing our understanding of communication pathways, especially in disease states. Here we evaluate the enrichment of the plasma membrane proteome utilizing the nanowire pellicle technique. The pellicle is constructed with iron silicate or silica core nanowires to observe the effects of wire density upon enrichment success. Comparison of these two wire pellicles reveals a two-fold enrichment of transmembrane proteins, over a multiple myeloma whole cell lysate, in both samples, with a slightly higher trend in the iron silicate nanowire pellicle. A covalent tagging method was also undertaken to assess its potential application to the study of myeloid-derived suppressor (MDSC) cell surfaces. This method couples glycan oxidation with biotinylation and enrichment on immobilized streptavidin to isolate surface glycoproteins. Application of this method to myeloid-derived suppressor cells yielded cell surface enrichment values ranging from approximately 50-60%. Furthermore, several protein groups of interest were identified for further assessment.

Development of Techniques for Plasma Membrane and Cell Surface Enrichment

By

Rebecca L. Rose

Thesis submitted to the Faculty of the Graduate School of the University of Maryland, College Park in partial fulfillment of the requirements for the degree of Master of Science
2014

Advisory Committee:
Professor Catherine Fenselau, Chair
Professor Douglas Julin
Professor Nicole LaRonde-LeBlanc
Professor Shuwei Li

Dedication

This work is dedicated to my parents, Michael and Jacqueline Rose. Without your love and support none of this would have been possible.

Acknowledgements

I would like to thank Dr. Catherine Fenselau for her unending guidance and support. Having the opportunity to work in her lab and learn from her vast knowledge and experience has been a wonderful opportunity and has shaped my thinking as a scientist. I also want to thank Dr. Yan Wang, director of the proteomics core facility, for her advice and expertise in liquid chromatography and LC-MS/MS. In addition I would like to thank Dr. Nathan Edwards for his advice in bioinformatic data processing and Dr. Peter Gutierezz for his guidance in cell culture. Finally I would like to thank Tim Maugel, the director of the Laboratory for Biological Ultrastructure, for his assistance in SEM sample preparation, and to acknowledge the Maryland Nanocenter and its NispLab for the use of their instrumentation for the capture of SEM images.

I would also like to acknowledge the members of the Fenselau Group: Dr. Joe Cannon, Dr. Avantika Dhabaria, Sitara Chauhuan, Amanda Lee, Lucia Geis, and Yeji Kim for their support. I would especially like to thank Dr. Waeowalee Choksawangkarn and Megahan Burke for their friendship and guidance during the last 3.5 years.

Lastly, I would like to thank my parents, Michael and Jacqueline Rose, and my sister Tessa Rose. Your love and support throughout my life have been a source of strength and encouragement, for which I am always grateful. Finally, I thank Justin Matoska for being a home away from home.

Table of Contents

List of Tables

List of Figures

List of Abbreviations

AAO	Anodic aluminum oxide
CD	Cluster of differentiation
DTT	Dithiothreitol
FBS	Fetal bovine serum
IAA	Iodoacetamide
ISNW	Iron silicate nanowires
LC-MS/MS	Liquid chromatography tandem mass spectrometry
LTQ	Linear ion trap
MDSC	Myeloid-derived suppressor cell
MS2	Fragment ion spectrum
MS/MS	Fragment ion spectrum
PAA	Poly(acrylic)acid
PBS	Phosphate buffered saline
PM	Plasma membrane
PMCB	Plasma membrane coating buffer
PNGase F	Peptide-N-glycosidase
RCDC	Reducing agent and detergent compatible
SDS	Sodium dodecyl sulfate
SEM	Scanning electron microscopy
TM	Transmembrane

Chapter 1: Introduction

The majority of initial communication occurring between cells and their external environment must begin at the cell surface. Therefore the cell surface plays a vital role in cell-to-cell, cell-to-vesicle, and more generally cell-to-biomolecule contact within the extracellular milieu. The central role of the surface proteome in communication makes it an ideal candidate for the development of potential drug targets[1]. While the surfaceome presents a strong target proteome, it is not necessarily a highly abundant one[2,3]. Therefore, the ability to study cell surface proteins is greatly diminished when one simply analyzes a lysate from a cell type of interest[2,3]. To accurately analyze the surface and plasma membrane proteins enrichment techniques must be employed to increase the presence of these proteins within a sample[2,3].

To this end a number of techniques have been developed over the years to better enrich the plasma membrane, or more generally, the cell surface, proteome. These techniques typically seek either to separate cellular components via altered density or chemical probing[2,3]. Both of these methods take advantage of the exposure of the cell surface while a cell remains intact. The addition of denser coatings to the plasma membrane allows for a more complete separation of this component from the remaining cellular debris upon lysis[4]. This coating has been dubbed a pellicle and was originally developed in the early 1980s[4]. Here we expound upon this technique to improve the enrichment it yields. Our new nanowire method will be elaborated upon within the studies reported in chapter 2.

In addition to utilizing density as a method of separation, many chemical probing techniques have also been developed to isolate the surfaceome. Some of these methods include: alkylation of lysine residues followed by biotinylation, which yields , lectin affinity columns, and oxidation of surface glycans followed by biotin tagging[5-10]. Each of these probe techniques takes

advantage of the exposure of glycan moieties and amino acid residues at the cell surface. Of the labeling techniques mentioned the coupling of oxidation with biotin tagging has yielded the most robust enrichment results[5-9]. With this information we chose to apply this method to a cell line of interest, myeloid-derived suppressor cells (MDSC), to conduct a qualitative study of their surfaceome. In addition to offering a substantial enrichment, the biotin tagging technique has the added advantage of utilizing the sugar residues as their target. Many groups have suggested the majority of surface proteins contain some type of glycan decoration[5-9]. Therefore, a tagging technique based upon the oxidation and covalent linkage to glycan residues is likely to capture a large number of surface proteins, thus offering a more complete and specific proteomic picture of the cell surface.

The objective of these studies is to apply and assess the viability of two surface enrichment techniques: pellicle coating with nanowires and oxidation/biotinylation tagging. Each of these techniques will be applied to cells within a proteomic workflow to assess their usefulness as enrichment methods. Within the pellicle study several types of wires and coating strategies will be employed and compared to assess if wire composition and density has an effect upon enrichment. The biotin tagging system has been well vetted and documented within the literature. Here we have adapted a protocol to apply to the MDSC for study of their surfaceome and identification of target proteins that may elucidate communication mechanisms within the tumor microenvironment. By analyzing both of these techniques we hope to develop the best method for interrogation of the surfaceome. This method may be applied to other cells and inhabitants of the tumor microenvironment to further interrogate and elucidate methods of communication within this disease state.

Chapter 2: Comparison of Iron Silicate to Silica Core Nanowire Pellicles for Plasma Membrane Enrichment in Multiple Myeloma Cells

Introduction

The study of plasma membrane (PM) proteins has long been an area of particular interest. Often PM proteins play key roles in signaling and other communication processes. As such, they are a proteome that has the potential to yield many therapeutic targets across disease types[1]. In response to this interest, many techniques have been developed for the isolation and study of the PM proteome. The technique of focus here is the pellicle method. This method was first developed by Jacobson and Chaney in 1983 and bases PM separation on the construction of a dense pellicle[4]. The original method used cationic silica beads, followed by cross-linking with anionic polymer to create the pellicle coating of the plasma membrane[4]. Following coating and cell lysis, the denser pellicle coated PM could be separated from the remaining cellular components via centrifugation[4]. This method was modified by Rahbar and Fenselau and placed in-line with a proteomic analysis to allow for the study of an enriched plasma membrane proteome[11].

Once isolated and analyzed via mass spectrometry, the success of the enrichment is measured by the assessment of the percentage of PM proteins identified within the sample. This value is compared to a whole cell lysate to ascertain the level of increased PM protein enrichment[12-16]. A second assessment can be performed by cataloguing the number of transmembrane (TM) domain-containing proteins identified in the pellicle sample[12-16]. These proteins are an even better metric for estimating enrichment of the PM proteome because they must contain a region that exists for the purpose of spanning the plasma membrane[15]. Furthermore, often PM proteins are misrepresented within the current proteomic databases, while

TM proteins are specifically categorized based on this characteristic. Therefore, using both categories to ascertain enrichment gives a more holistic view of the pellicle-enriched sample.

Many subsequent experiments have been performed to attempt to improve pellicle construction[12-17]. There have been several attempts to create a pellicle that leads to better PM separation by utilizing particles of a higher density[12-15]. A natural extension of this is to attempt pellicle construction using a nanowire. Nanowires offer the opportunity for an even more-dense pellicle due to their size and myriad of core possibilities. In addition, nanowires offer far more points of contact along the cell surface, and thus have the potential to create a much stronger pellicle that can lead to a more complete separation of the PM from the remaining cellular debris[17,18]. This work seeks to assess the viability of nanowires as pellicle constructive materials. Furthermore, it seeks to compare the success of PM enrichment when higher (iron silicate core) and lower density (silica core) nanowires are applied to the pellicle. The nanowire coating will be evaluated via scanning electron microscopy (SEM), and the success of plasma membrane separation and enrichment will be evaluated based upon both PM and TM protein identifications following proteomic analysis using mass spectrometry.

Materials and Methods

Materials

Materials for the construction of both iron silicate and silica nanowires were obtained and utilized by the Lee lab. For all a Milli-QA10 system supplied the deionized water. Iron (III) chloride ($FeCl_3$*$6H_2O$, 97.0%) was purchased from Alfa Aesar (Ward Hill, MA). Anodic aluminum oxide (AAO) templates of 60nm thickness, and containing pores of approximately 200nm, were purchased from Whatman GmbH (Dassel, Germany). The cells utilized for coating were a human multiple myeloma cell line RPMI 8226, grown in RPMI 1640 media both

purchased from American Type Culture Collection (Manassas, VA). Sodium dodecyl sulfate (SDS), beta-mercaptoethanol, Tris-HCl, KCl, urea, gluteraldehyde, ammonium bicarbonate, poly(acrylic)acid (PAA), NaCl, imidazole, D-sorbitol, sodium carbonate, dithiothreitol (DTT), protease inhibitor cocktail, iodoacetamide (IAA), 2-(N-morpholino)ethanesulfonic acid (MES), tetraethylorthosilicate, and penicillin-streptomycin antibiotic solution were procured from Sigma-Aldrich (St. Louis, MO). Fetal bovine serum was purchased from Atlanta Biologicals (Lawrenceville, GA). Protein assay kits used were RC DC kits purchased from Bio-Rad (Hercules, CA). The proteases used were mass spectrometry grade Lys-C and trypsin obtained from Promega (Madison, WI). The C18 TopTips were procured from Glygen Corp (Columbia, MD). Solvents utilized for LC-MS/MS: acetonitrile, formic acid and trifluoroacetic acid were purchased from Thermo Fisher Scientific (Pittsburgh, PA). The laboratory grade microwave utilized for protein extraction was purchased from CEM Corporation (Matthews, NC). The liquid chromatography system used for sample analysis was a Shimadzu Prominent nanoHPLC (Shimadzu BioSciences, MD), which was in-line with a Thermo nano-electrospray ionization source and an LTQ-Orbitrap XL (Thermo Fisher Scientific, CA).

Nanowire synthesis

The nanowire synthesis was performed in the Lee lab utilizing the following conditions taken from our previous publication on the use of nanowires for plasma membrane analysis:

"Silica and iron silicate nanowires were synthesized through a sol-gel evaporation process as described in our previous work (Kim et al. 2013). Briefly, for silica nanowires, 1 M TEOS solution was prepared by adding 2.08 g tetraethyl orthosilicate (TEOS) to 3.95 g ethanol, 1.8 g water, and 3 g of 0.2 M HCl. The solution was hydrolyzed at 60 ^{o}C for 1 hr, followed by immersing commercial AAO templates into properly adjusted amounts of the solution and drying

at room temperature for 6 hrs then at 120 ^{o}C for 24 hrs, sequentially. The synthesis of ISNW followed the same process using a modifying TEOS solution of 1.35 g $FeCl_3 \cdot 6H_2O$, 1.04 g TEOS, 3.95 g ethanol, 1.86 g H_2O, and 1.5 g of 0.2 M HCl. After sol-gel synthesis, the AAO templates were dissolved in 0.1 M sodium hydroxide to release free-standing nanowires. After washing these 60 µm nanowires several times with DI water, a sonicator equipped with a microtip (Q500, QSONICA, LLC., CT) was employed to cut the nanowires into shorter pieces.

To cover the surface with an alumina layer, the nanowires were dispersed in 0.01 M $Al(NO_3)_3$/0.1M $K(NO_3)$ solution for 24 hrs. After rinsing with water, the alumina-coated nanowires were dispersed in PMCB solution (see below) for prompt use in cell coating experiments. The nanowires were characterized by using a Hitachi SU-70 Field Emission SEM (Hitachi High-Technologies America, Inc., Gaithersburg, MD) and a JEOL JEM-2100F Field Emission TEM (JEOL USA, Inc., Peabody, MA) operating at 200 kV with scanning TEM capability and Oxford energy dispersive x-ray spectrometry, and a Zetasizer Nano ZS90 particle analyzer (Malvern Instruments Ltd, Worcestershire WR14 1XZ, UK)."[17,18]

Pellicle construction

The protocol utilized for pellicle construction was adapted from the previous protocol developed by Rahbar and Fenselau as discussed in our current publications of this method development. [11,17,18] Human multiple myeloma cells of the RPMI 8226 cell line were grown at 5% CO_2 in RPMI 1640 media containing 5% FBS and 1% antibiotic solution at 37°C. Cells were counted via hemocytometer and a volume containing $1x10^8$ cells was collected for coating. All coating experiments were performed in parallel with the only change being the wire type utilized in pellicle construction: iron silicate vs. silica. After cell collection, cells were washed three times for five minutes at 900xg in 10 mL of plasma membrane coating buffer (PMCB, 800 mM

sorbitol, 20 mM MES, 150 mM NaCl, pH 5.3). Following washing cells were resuspended in 2mL of PMCB and added dropwise to the suspended nanowires. Coating occurred for 15 minutes at 4°C gently rocking. Following the coating incubation, cells were pelleted from the wires via centrifugation as described above. The coated cells were washed three times with PMCB as performed previously. The final cell pellet was again resuspended in 2 mL of PMCB and added dropwise to a 10% w/v solution of PAA and incubated for crosslinking at 4°C, rocking for 15 minutes. The coated and cross-linked cells were removed and washed as after the coating step and finally resuspended in 10 mL of lysis buffer (2.5 mM imidazole with protease inhibitor cocktail). Cells were incubated in lysis buffer for 30 minutes at 4°C, followed by 30 minutes incubated under nitrogen at 1800 psi. Following lysis a small aliquot was taken and visually inspected via optical microscope to determine the thoroughness of lysis. The pair of incubations was repeated twice more to ensure approximately 80% cell lysis by visual inspection. Figure 1 is a visual schematic of the entire coating process as described above.

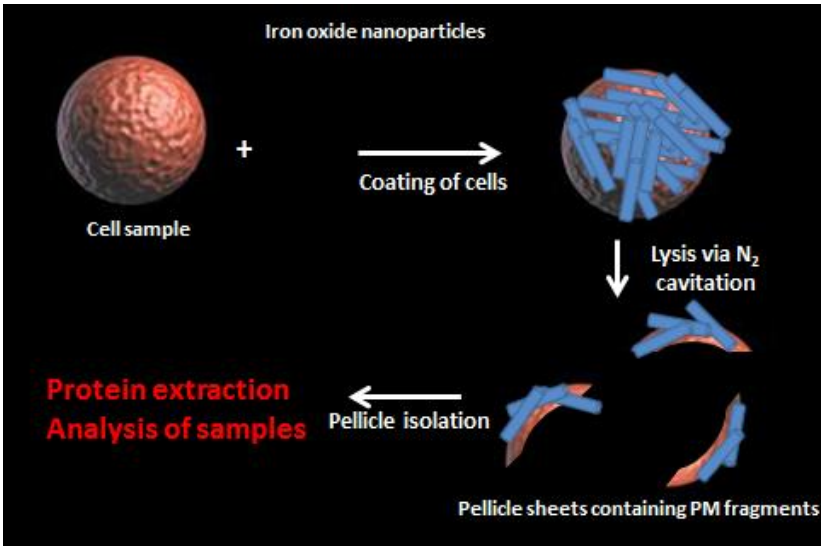

Figure 1. A schematic representation of the coating of multiple myeloma cells with nanowires, followed by lysis and separation of the pellicle fragments for analysis.

After complete lysis the pellicle fragments were separated from the remaining cellular debris via serial, low speed centrifugation washes. In total, nine washes for 7 minutes at 100xg were performed. The first three utilized lysis buffer, followed by 1 M sodium carbonate and finally 1 M KCl. Proteins were extracted from the pellicles via microwave assisted extraction. The pellicle was resuspended in 2% SDS, 62.5 mM Tris-HCl, and 5% beta-mercaptoethanol. The samples were incubated in a laboratory grade microwave for 5 minutes at 100ºC to allow for rapid protein extraction. This extraction was performed a total of three times and the samples assayed using an RC DC protein assay kit. If needed, samples were pooled to yield 100 µg of starting material. It should be noted that for all experiments in which cross-linking was not performed the only deviation from the above protocol was the absence of the incubation with PAA for cross-linking.

Confirmation via scanning electron microscopy (SEM)

During each step of the coating experiment a small aliquot of sample was preserved for SEM analysis. Each sample set included the following: intact bare cells, wire coated cells, coated and cross-linked cells, and finally lysed cells. Thus, for each parallel experiment seven samples were kept for SEM analysis. Each sample was fixed with 2% glutaraldehyde in 0.12 Millonig's phosphate buffer at pH 7.3 overnight at 4°C. The day of sample preparation, samples were moved to a 1% osmium tetroxide secondary fixing solution. Secondary fixing was performed for one hour. Subsequently cells were subjected to five serial 30 minute drying steps using ethanol ranging in concentration from 75%-100%. A Denton DCP-1 critical point dryer was used for the final drying step. Dried samples were coated in a DV-503 Denton Vacuum evaporator with Au:Pd at a ratio of 15nm of coating per sample. Images were taken on a Hitachi SU-70 Field Emission SEM.

Analysis via mass spectrometry

Following protein extraction, approximately 100 µg of protein was precipitated using chloroform: methanol precipitation. Once precipitated the proteins were resuspended in 8 M urea and 50 mM ammonium bicarbonate. Following thorough solubilization of the precipitated pellet, proteins were reduced with 20 mM DTT for 30 minutes at 56°C and subsequently alkylated with 40 mM IAA for 30 minutes in the dark at room temperature. Samples were diluted to a 1.6M urea concentration in 50mM ammonium bicarbonate and digested at 37°C for 3 hours with Lys-C. Following this digestion, samples were incubated for 16 hours with trypsin. The resulting peptide samples were desalted using C18 TopTip spin columns and peptides were recovered in 85% acetonitrile, 0.1% formic acid. These samples were dried via lyophilization and resuspended in 0.1% formic acid for analysis via LC-MS/MS.

The samples were analyzed via a Shimadzu Prominent nanoHPLC in line with an LTQ-orbitrap XL. Five replicate injections of 15 µg of protein per injection were performed. Each sample was trapped using a Zorbax 300SB-C18 column (0.3x5mm) using solvent A (97.5% water, 2.5% acetonitrile, 0.1% formic acid) at a flow rate of 10ul/minute. An EVEREST C18 column, comntaining 300A pores and 5 µm particles, was used to fractionate the samples. The samples were fractionated at a flow rate of 500 nl/minute using a 120 minutes linear gradient of 5% solvent B to 40% solvent B (97.5% acetonitrile, 2.5% water, 0.1% formic acid), followed by 25 minutes incrasing solvent B from 40% to 80%. Samples were injected into the nano-electrospray ionization source via a 15 µm PicoTip. Instrument parameters were as follows: spray voltage- 2kV, capillary temperature 275°C, peptide precursor resolution at 400m/z-30,000, number of ions fragmented- the nine most abundant precursor ions, normalized collision energy 35, activation time 30ms, and isolation window 3Da. During the run dynamic exclusion

was utilized at a window of 3 minutes, in addition only ions with a charge of +2 or higher were sent for fragmentation.

Bioinformatics

All data acquisition files were stored using Thermo Xcalibur 2.0 (Thermo Fisher Scientific, CA). These .RAW files were reformatted to an mxXML format and uploaded to an in-house search program called PepArML, which utilizes seven search engines (Mascot, Tandem, OMSSA, KScore, SScore, Myrimatch, and InsPecT) to search again the UniProtKnowledgebase (March 2012 version)[19]. Searches were performed using the following parameters: enzyme cleavage- tryptic, variable modifications- oxidation of methionine, fixed modifications- carbamidomethylation of cysteine. Protein identifications were required to have two or more unique peptides, with an overall false discovery rate of 10% or less. Special attention was paid to transmembrane proteins as potential indications of success and these were assigned against the UniProtKnowledgeBase keyword annotation. In addition to utilizing protein annotation as a measure of enrichment, spectra counting was also performed using an in-house program (Spectral Count) made by Dr. Nathan Edwards. The program compares the number of spectra contributed by each protein as another measure of its abundance within the overall proteome.

Results and Discussion

Comparing the effect of wire type upon coating success

In choosing to coat the cells with nanowires we hoped to capitalize on creating a stronger pellicle through multiple points of contact between the wire and the cell. One of the final steps in nanowire construction is the cutting of larger wires into the desired nanometer range for our coating purposes. This cutting is achieved via sonication and thus does not yield a uniform sized wire product, but rather a range of wire lengths. The size range achieved for each wire type is

depicted in Figure 2. From this figure, we observe the silica nanowires to have a broader distribution of wire lengths, with a trend toward longer wires than the iron silicate nanowires. The longer silica wires can be attributed to the inherently tougher quality of the silica core. This core makes the wires more difficult to cut, and results in longer wire lengths. Thus the question is raised: will wire length affect coating, and in turn will this affect pellicle fragment size and separation from the remaining cellular debris?

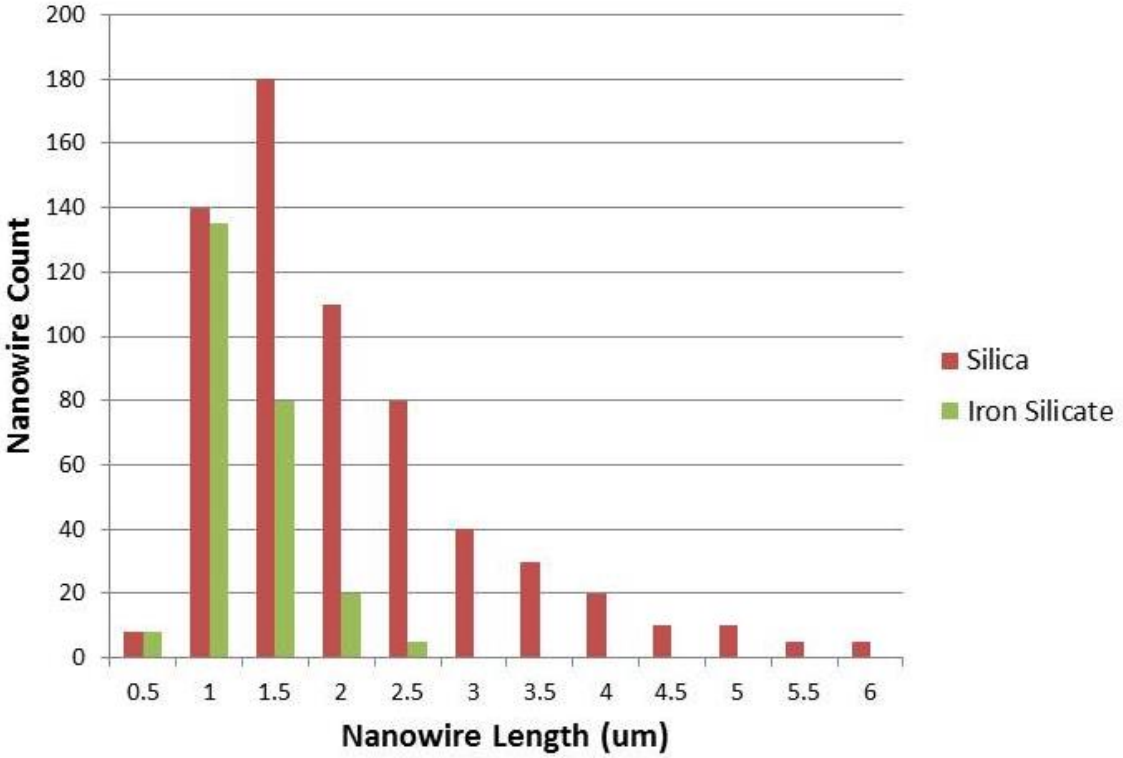

Figure 2. Comparison of the range of wire lengths achieved in the construction of nanowires for PM pellicles. The silica wires trended towards a longer length and typically proved more challenging to cut.

Visual inspection and comparison of coating was performed through SEM image capture and analysis. SEM images were taken of samples reserved throughout each coating experiment to determine the success of coating in a visual and qualitative manner. The SEM images found in Figure 3 are of an iron silicate nanowire coating and cross-linking experiment. The iron silicate nanowires very thoroughly coat the cells in several layers (3B). It appears the shorter length of

the iron silicate nanowires allows them to layer together tightly along the cell surface, and to follow the curvature of the cell more completely in the pellicle construction. The addition of PAA does not cause any detrimental effects to coating, but does causes loose wires in solution to aggregate (3C). However, a multilayered coating is maintained in the presence of cross-linking. Upon lysis of the cells a range of fragment sizes were found (3D). During lysis it appeared the PAA aided in maintaining pellicle attachment (3F), however the absence of PAA appears to have resulted in bare pellicle fragments (3E).

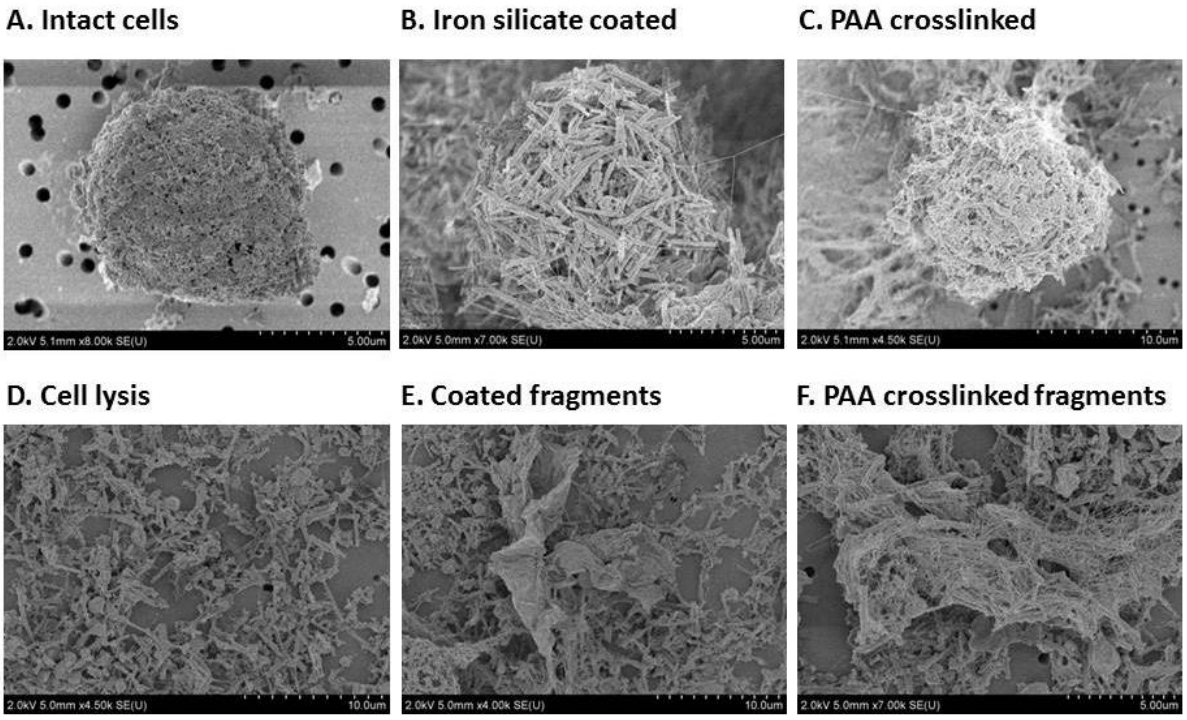

Figure 3. SEM images of multiple myeloma cells during each step of coating with iron silicate nanowires. A. intact cell, B. iron silicate nanowire coated cell, C. coated and cross-linked cell, D. cell lysis, E. single pellicle fragment after lysis without cross-linking, F. pellicle fragments after lysing with cross-linking.

Pellicle construction with silica wires was also successful as can be seen in the SEM images of Figure 4. The silica wires were able to coat the cells and create a fairly strong layer. It should be noted that comparatively, the silica wires do not create as thick a layer as the iron

silicate nanowires (4B). There are portions of the cell surface without thorough coating. These are indicated by a thinning of wire coverage and a change in layering of nanowires. It is possible the longer silica nanowires are not able to pack as tightly against the cell surface. In addition, their rigid character might prevent longer wires from curving to interact with the cell surface. Cross-linking appears to fill some gaps made by incomplete coating and results in a thicker pellicle (4C). Upon lysis, fragments appear to be smaller than those yielded by iron silicate nanowire coating (4D). However, there are examples of larger portions of pellicle following lysis (4E and F).

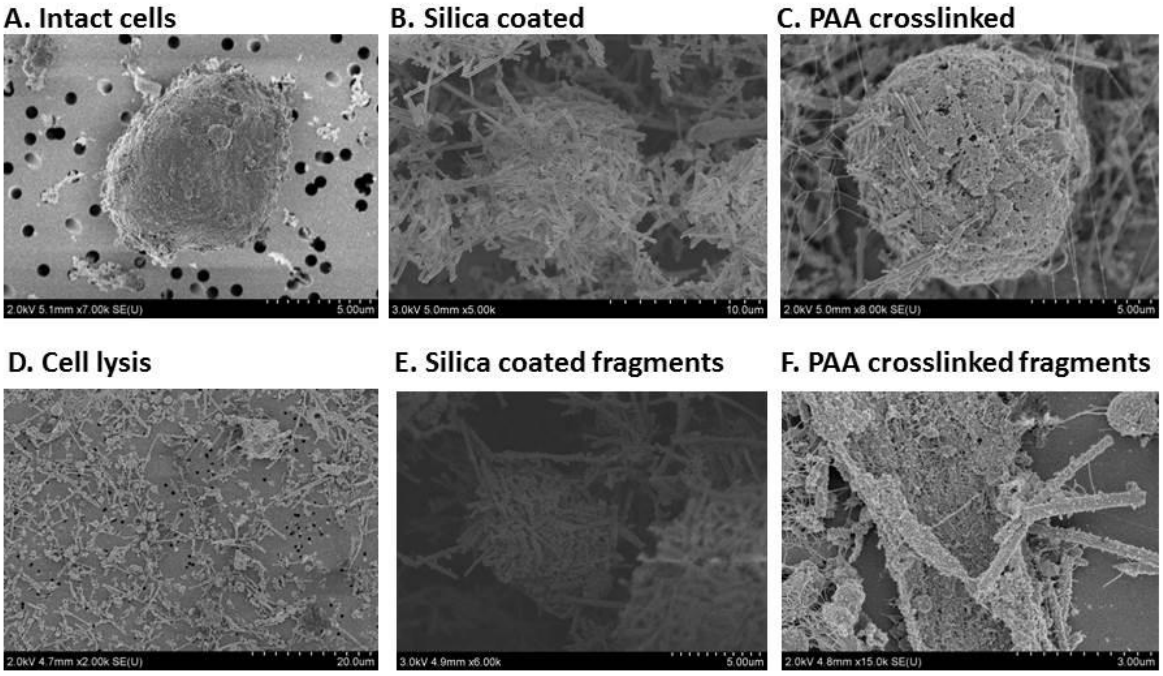

Figure 4. SEM images of multiple myeloma cells during each step of coating with silica nanowires. A. intact cell, B. silica nanowire coated cell, C. Coated and cross-linked cell, D. Post-lysis, E. Closer look at pellicle fragments without cross-linking, F. Fragments with cross-linking.

In addition to using SEM images to confirm successful coating utilizing both wire types, a semi-quantitative comparison was performed between several samples. Namely, we assessed the presence or absence of a correlation between pellicle construction methods and fragment size

range or extent of cell lysis. In comparing wire types to the extent of cell lysis we found that both wire types are comparable (5A). As can be seen in Figure 5A the number of unlysed cells is very similar between cells coated with iron silicate or silica nanowires. This suggests the wires themselves do not differ greatly in their effect upon pellicle firmness. However, when cross-linking is removed from the pellicle construction it appears the pellicle does become more malleable and the number of unlysed cells decreases. This suggests that it is the presence of PAA that affects the firmness of the pellicle, rather than the type of wire used. To further explore the effect of cross-linking upon pellicle fragments a comparison of approximate fragment sizes to the presence or absence of cross-linking was performed on the iron silicate nanowire pellicle (5B). It was found that when the pellicle was constructed without cross-linking the resulting fragments trended towards a smaller size than those resulting from a cross-linked pellicle (5B). This further supports the notion that cross-linking has an effect upon pellicle construction and resistance to lysis conditions.

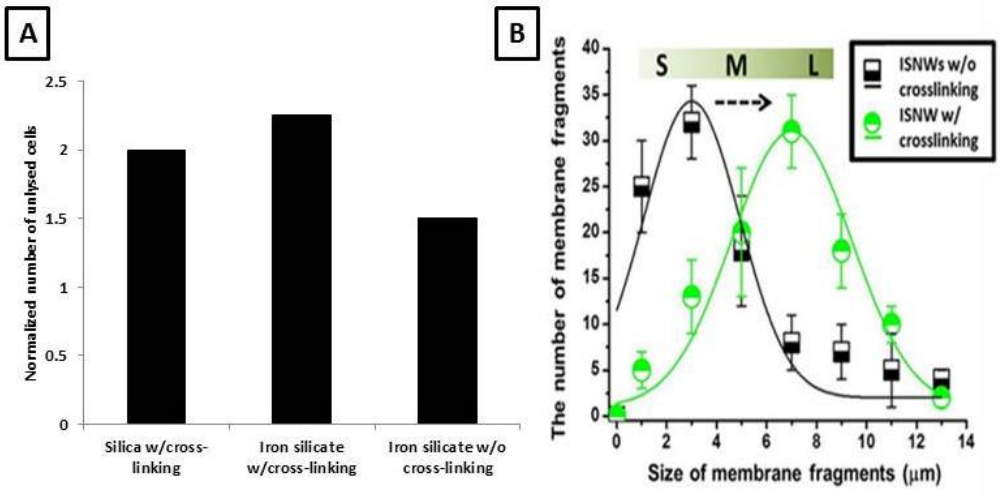

Figure 5. An assessment of unlysed cells after coating with each wire type, with or without PAA crosslinking (A). The distribution of pellicle fragment sizes iron silicate nanowires with (green) and without (black) crosslinking (B).

While the visual inspection of SEM images offers a confirmation of the success of coating, a proteomic analysis is required to truly assess the usefulness of nanowire pellicles as a technique for isolating the plasma membrane for study. For each iron silicate nanowire four biological replicates were performed: two with pellicle construction including cross-linking, followed by two without cross-linking. These were done in parallel with the silica nanowire counterparts. For each experiment plasma membrane and transmembrane protein enrichment was assessed as compared to a whole cell lysate (Table 1). It was found that the enrichment of the plasma membrane was not particularly successful when compared to other techniques. In comparing the results across replicates it can be observed that the cross-linked samples have slightly higher enrichment values than that of the non-cross-linked samples. This correlates to the fragment size distribution shown in figure 5B, as the ideal pellicle fragment will be slightly larger and thus more easily separated from cellular debris.

In comparing the transmembrane enrichment values we see a two fold increase over the cell lysate values. This is a more promising indication of pellicle success, and a more accurate representation of the plasma membrane proteome. The transmembrane assignment was made using a web-based program THMM2.0, which bases the transmembrane assignment upon predicted helices yielded by protein structure.[33] Those proteins containing transmembrane domains are most certainly considered to be plasma membrane proteins, while the annotated term plasma membrane becomes a much more amorphous characterization in the UniProtKnowledgeBase. These assignments are often inconsistent and may result in mis-assignment of plasma membrane proteins. Thus, the lower plasma membrane enrichment values may be attributed to a miss annotation of proteins identified, while the transmembrane enrichment is a more definitive characterization of the proteome isolated by the pellicle. In

taking this line of reasoning, it can be said that the nanowire pellicle does isolate the plasma membrane from the remainder of the cell. In the case of cross-linking vs. not cross-linking it appears that for the transmembrane proteome there is less of a trend towards one condition over another. However, there is a slight decrease in the absence of cross-linking that again confirms the SEM observation of a more ideal pellicle size range being achieved with the presence of PAA.

In observing the trends across the silica nanowire replicates we observe lower enrichment in both the plasma membrane and transmembrane proteome (Table 2). Interestingly, there seems to be not trend in comparing the presence to absence of cross-linking. This suggests that perhaps the silica nanowire pellicle is not as well constructed as the iron silicate pellicle. It is possible that the silica wires do not maintain a well-constructed pellicle, and thus fall off during the lysis process. This would explain the lack of difference observed with and without cross-linking. If the pellicle does not remain firmly attached due to the wires, the difference in toughness created by PAA cannot be observed, as rather than creating a stronger pellicle most likely the cross-linking causes wire aggregation. This is supported by images 4D and 4E as we can observed small aggregates of silica nanowire and PAA post-lysis, which suggests they did not maintain contact with the plasma membrane to create pellicle sheets.

Sample ID	Total Protein IDs	IDs w/ GO Annotation	% Plasma Membrane	% Transmembrane
Iron silicate + PAA 1	615	587	18.0%	12.3%
Iron silicate + PAA 2	541	509	16.5%	11.4%
Iron silicate – PAA 1	364	317	16.1%	11.5%
Iron silicate – PAA 2	378	326	15.5%	10.2%
WCL (N=3)	658	589	15.0%	5.0%

Table 1. A summation of protein identifications, plasma membrane and transmembrane enrichment across four replicate iron silicate nanowire pellicle constructions. It should be noted two are with crosslinking (+PAA), while two are without (-PAA).

Sample ID	Total Protein IDS	IDs w/ GO Annotation	% Plasma Membrane	% Transmembrane
Silica + PAA 1	457	432	14.5%	11.1%
Silica + PAA 2	382	335	15.1%	10.5%
Silica – PAA 1	271	234	14.3%	10.0%
Silica – PAA 2	291	253	14.6%	10.2%
WCL (N=3)	658	589	15.0%	5.0%

Table 2. A summation of protein identifications, plasma membrane and transmembrane enrichment across four replicate silica nanowire pellicle constructions. It should be noted two are with crosslinking (+PAA), while two are without (-PAA).

A more direct comparison of the iron silicate vs. silica nanowires shows the overall success of the iron silicate wires to be slightly higher than the silica (Figure 6). As can be observed in the top panel of Figure 6, the iron silicate nanowires give higher plasma membrane enrichment

than the silica nanowires. In fact, both cross-linked and not cross-linked iron silicate nanowires perform more favorably than either type of silica nanowire. However, under all four conditions the plasma membrane enrichment does not rise far beyond that of the whole cell lysate condition. If we look to the transmembrane enrichment values as a more dependable indication of plasma membrane isolate, a different result emerges (Figure 6, bottom panel). Here we observe an approximately two fold increase in enrichment across the experiment conditions. This suggests that the nanowire pellicle does isolate the plasma membrane and its membrane-spanning proteome. Iron silicate nanowires do continue to perform more favorably, with both cross-linking conditions yielding a higher level of enrichment. These values, taken with the SEM images suggest that the iron silicate cross-linked samples offer the most stable pellicle construction and thus the most favorable pellicle sheets for isolation from cellular debris. Furthermore, in comparing the number of identifications made by each experiment type is should be noted that the iron silicate nanowires consistently yield more total protein identifications as compared to the silica nanowires (table 1 and table 2). Thus, with higher enrichment and a higher number of total proteins identified the iron silicate nanowires offer a larger data set of either transmembrane or plasma membrane proteins for analysis.

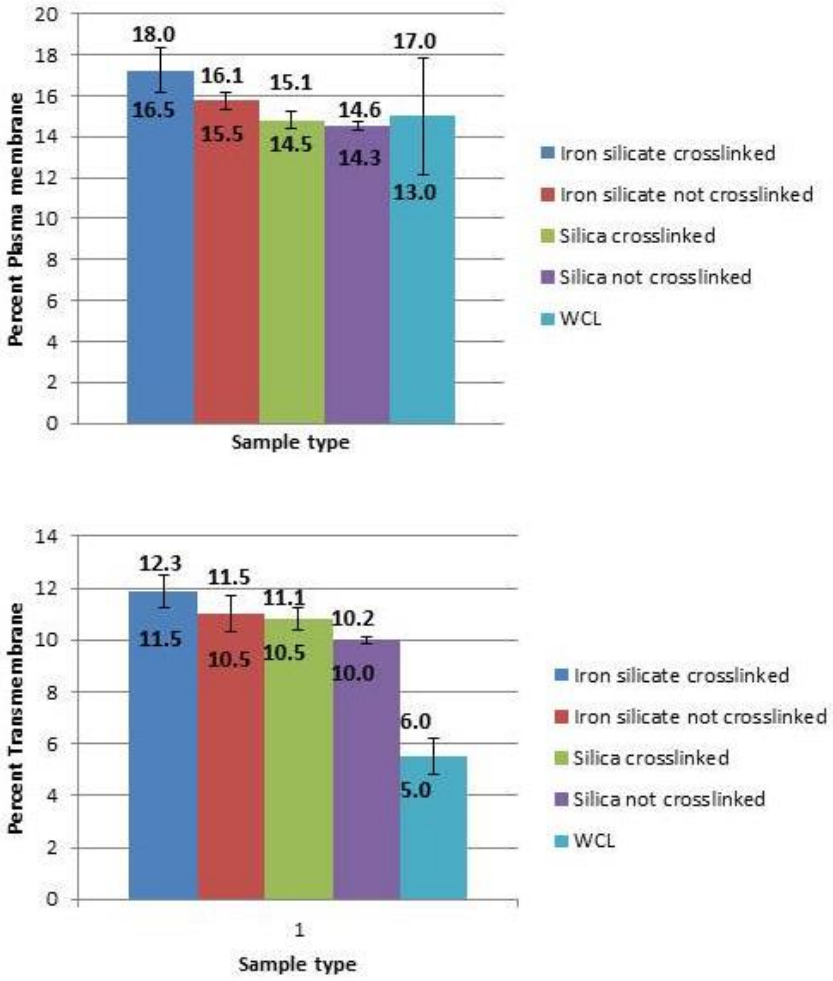

Figure 6. Comparative graphs of the plasma membrane (top) and transmembrane (bottom) enrichment across both wire types and in the presence or absence of cross-linking.

In addition to assessing pellicle isolation success using protein annotation and enrichment, we also used spectral counting to compare the enrichment values across all four experimental conditions. As mentioned above in the methods section, spectral counting accumulates the number of spectra contributed by each protein identified. Thus, protein abundance can be semi-quantitatively assessed to offer another estimate of enrichment of proteins from the plasma membrane or transmembrane cohort. Using this tool we assessed the enrichment of both of these protein annotations and found the values to be very similar to those given by assessing enrichment at the protein identification level (Table 3). There was slight decrease in the

presence of transmembrane proteins, however these proteins are typically lower in abundance within the cell and the values may simply be a reflection of this fact.

Sample ID	% Plasma Membrane (Std. Dev.)	% Transmembrane (Std. Dev.)
Iron silicate crosslinked	16.67 (0.16)	10.7(0.28)
Iron silicate not crosslinked	15.22 (0.33)	10.07(0.31)
Silica crosslinked	14.71 (0.07)	10.03(0.34)
Silica not crosslinked	14.02 (0.33)	9.31(0.78)

Table 3. Summation of enrichment values utilizing spectral counting rather than protein assignment. The data still shows very comparable values.

One final comparison of note is the comparison of identifications between wire types. In comparing the total identifications yielded by the cross-linked iron silicate nanowires to the cross-linked silica nanowires (7A) we observe that the proteins common to both experiments comprise approximately 50% of the iron silicate cohort and 79% of the silica cohort. This suggests that the majority of identifications from the silica experiment are also present in the iron experiment. The fact that the iron silicate nanowires have a higher percentage of enrichment and a large number of additional proteins suggests that these additional plasma membrane proteins are unique to the iron silicate sample, confirming once more that the iron silicate nanowires are the more successful pellicle construction material. If we turn to the comparison of the transmembrane region (7B) a different conclusion can be drawn. We can see that the majority of both samples are common identifications. This suggests that there is no real

difference in the isolation of the plasma membrane as indicated by the more dependable transmembrane identifications.

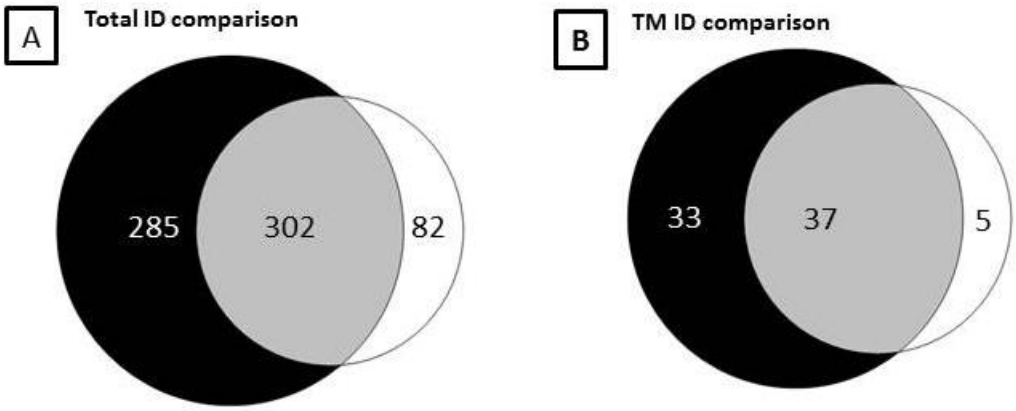

Figure 7. Comparison of total identifications (A) and transmembrane domain containing identifications (B) yielded from iron silicate (black) cross-linked vs. silica (white) cross-linked samples.

Conclusions

Both types of nanowire pellicle show promising results as a method for plasma membrane isolation. The ability of the nanowires to form multiple charge-charge interaction points with the cell surface allows for the formation of strong, multi-layer pellicles. In comparing the two types of wires it appears iron silicate nanowires tend to offer slightly improved enrichment values. This correlates to their smaller average length and ability to form more compact, fully coating pellicles (as shown via SEM imaging). However both wire types offer approximately twofold transmembrane domain containing protein enrichment, which suggests a well isolated plasma membrane fraction. Further capitalization on the strength of these pellicles may be achieved with the application of magnetic iron silicate nanowires as a more thorough method of separation after pellicle construction.

Chapter 3: Interrogating the Surface of Myeloid-Derived Suppressor Cells Using Glycoprotein Tagging

Introduction

Myeloid-derived suppressor cells (MDSC) are a subpopulation of immature myeloid cells (IMCs) that have not yet fully differentiated[20-25]. In healthy tissues, IMCs will become granulocytes, monocytes, or macrophages[20,21,22]. However MDSC exhibit incomplete expression of cell surface markers found on any of these cell types; thus, supporting the point that they are a heterogeneous population of immature cells[20-24]. The MDSC have been found to be potent suppressors of immune response via T cell suppression and inhibition of adaptive immune response in the lymph nodes[23-25]. Within a tumor microenvironment the accumulation of MDSC has been suggested as a response to the signaling of cytokines and other signal molecules associated with the cancerous state[20-25]. Of these, pro-inflammatory molecules secreted by the tumor have been shown to strongly recruit MDSC. Once within the tumor microenvironment, the MDSC also participate in self-recruitment, causing even greater enhancement to the tumor's immunosuppressive capabilities[20-25].

The occurrence of MDSC recruitment to the tumor microenvironment, as well as their immunosuppressive effects makes their surface one of particular interest for study. Presumably, any initial communication or signaling must occur at the cell surface level. Therefore, a greater understanding of the cell surface proteome of MDSC under inflammatory conditions may shed light on the communication pathways that are utilized[20-23]. Our collaborator, Dr. Suzanne Ostrand-Rosenberg, has created a mouse model containing a pro-inflammatory tumor microenvironment by injecting BALB/c mice with a 4T1 mammary carcinoma that has been transfected with the interleukin-1β gene[22-25]. The tumor microenvironment created within these

mice contains increased amounts of the cytokine interleukin-1β, and thus is considered to be a pro-inflammatory environment[22-25].

To study the surface proteome of the MDSC recruited to this tumor microenvironment, we chose to utilize a chemical tagging system that targets surface glycans. This system is a two-step reaction in which surface glycans are oxidized and subsequently bound to a biotin tag via aminooxy chemistry[5-9]. Once tagged, the proteins can be removed from the remaining cellular components via on-column enrichment with streptavidin (Figure 8). This system is well-suited to our purpose as it has been stated that the majority of cell surface proteins are believed to have some type of glycosylation added to their structure[5-9]. These charged, or at the very least polar, glycan residues may play a key role in the communication pathways utilized by MDSC within the tumor microenvironment[22-25]. Thus, the enrichment of this glycosylated surface proteome allows for the direct targeting of those proteins in which we have an interest. The goals of these experiments is to determine if this tagging system is an effective enrichment technique, as compared to the pellicle, and to isolate specific proteins of biological relevance both for our own study and our collaborator's.

Materials and Methods

Materials

For all experiments water used was obtained from a Milli-Q A10 system. Ammonium bicarbonate, glycerol, SDS, Triton X-100, sodium(meta)periodate, protease inhibitor cocktail, urea, DTT, iodoacetamide, aniline, PBS, and Tris-HCl were all purchased from Sigma-Aldrich (St. Louis, MO). Fetal bovine serum (FBS) was purchased from Atlanta Biologicals (Lawrenceville, GA). Trypsin was purchased from Promega (Madison, WI). PNGase F and its associated G7 buffer were purchased from New England Biolabs (Ipswich, MA). NaCl was

purchased from EMD chemicals (Gibbstown, NJ). Aminooxy-biotin was purchased from Biotium (Hayward, CA). High capacity streptavidin beads were purchased from Thermo Scientific (Rockford, IL). Solvents utilized for LC-MS/MS: acetonitrile, formic acid and trifluoroacetic acid were purchased from Thermo Fisher Scientific (Pittsburgh, PA). The C18 TopTips were procured from Glygen Corp (Columbia, MD). The liquid chromatography system used for sample analysis was a Shimadzu Prominent nanoHPLC (Shimadzu BioSciences, MD), which was in-line with a Thermo nano-electrospray ionization source and an LTQ-Orbitrap XL (Thermo Fisher Scientific, CA).

The Collection of MDSC

The mammary fat pads of BALB/c mice were injected with the 4T1 mammary carcinoma that had been transfected with the Il1-β gene to create a tumor microenvironment with elevated levels of inflammation[22-25]. Following the establishment of metastasis the MDSC were harvested in blood via tail prick. MDSC were purified via centrifugation and flow cytometry to over 95%.

Biotinylation and On-column Enrichment

The following protocol was adapted from previously published biotin tagging methods (Figure 8)[9]. The MDSC were washed twice with phosphate buffered saline (PBS) containing 5% FBS at pH 7.4, via centrifugation at 900xg for 5 minutes. Surface glycans were oxidized via cell resuspension in 1mM sodium periodate in PBS with 5% FBS and incubation for 20 minutes at 4°C. The oxidation reaction was halted via the addition of glycerol to a final concentration of 1mM. Subsequently, two washes, as previously described, were performed. Glycans were biotinylated for 1 hour at 4°C in 100uM aminooxy-biotin in the presence of 10mM aniline in PBS with 5% FBS buffered to pH 6.7[5]. Following biotinylation cells were washed twice, as described previously, and resuspended in lysis buffer (150mM NaCl, 5mM iodoacetamide,

10mM Tris-HCl, and protease inhibitor cocktail) at 4°C for 30 minutes to overnight when needed to reach approximately 70% lysis upon inspection via light microscopy.

Streptavidin beads were loaded onto snap cap spin columns, and equlibrated via two washes with lysis buffer, each terminated by centrifugation at 500xg for one minute. Cell lysates were spun twice at 2800Xg for ten minutes and twice at 16,000xg for ten minutes to remove nuclear and subcellular organelle material. Supernatants containing biotinylated glycoproteins were incubated on 50ul of streptavidin beads for 2 hours at 4°C. Following incubation, columns were spun at 1,000xg for one minute to remove non-bonded residual protein and cellular material. Bound proteins were washed on-column with lysis buffer followed by PBS containing 0.5% SDS via centrifugation at 1,000xg for 1 minute each. Proteins were reduced with 100mM DTT and 0.5% SDS, in PBS, and alkylated on-column via 50mM iodoacetamide, in UC buffer (6M urea, 100mM Tris-HCl), for 20 minutes at room temperature respectively. Proteins were washed with 600ul of UC buffer, PBS and water via serial centrifugation spins at 1,000xg for one minute per spin.

On-column tryptic digestion was performed overnight using 4ug of trypsin suspended in 50mM ammonium bicarbonate. The following morning tryptic peptides were eluted via centrifugation at 1,000xg for one minute and washed with ammonium bicarbonate in the same manner. The elution and wash fractions were pooled as one tryptic peptide fraction. Columns were then washed with PBS, water and G7 buffer (50mM sodium phosphate) via serial centrifugation as described previously. Samples were incubated overnight with 15,000 units of PNGase F in G7 buffer at 37°C. This incubation released those peptides directly attached to the biotinylated surface glycans. Glycopeptides were eluted the following morning, washed with G7 buffer and pooled in the same manner as the tryptic peptide fraction. Both fractions were

cleaned up via C18 spin column, lyophilized, and resuspended in 0.1% formic acid for LC-MS/MS analysis.

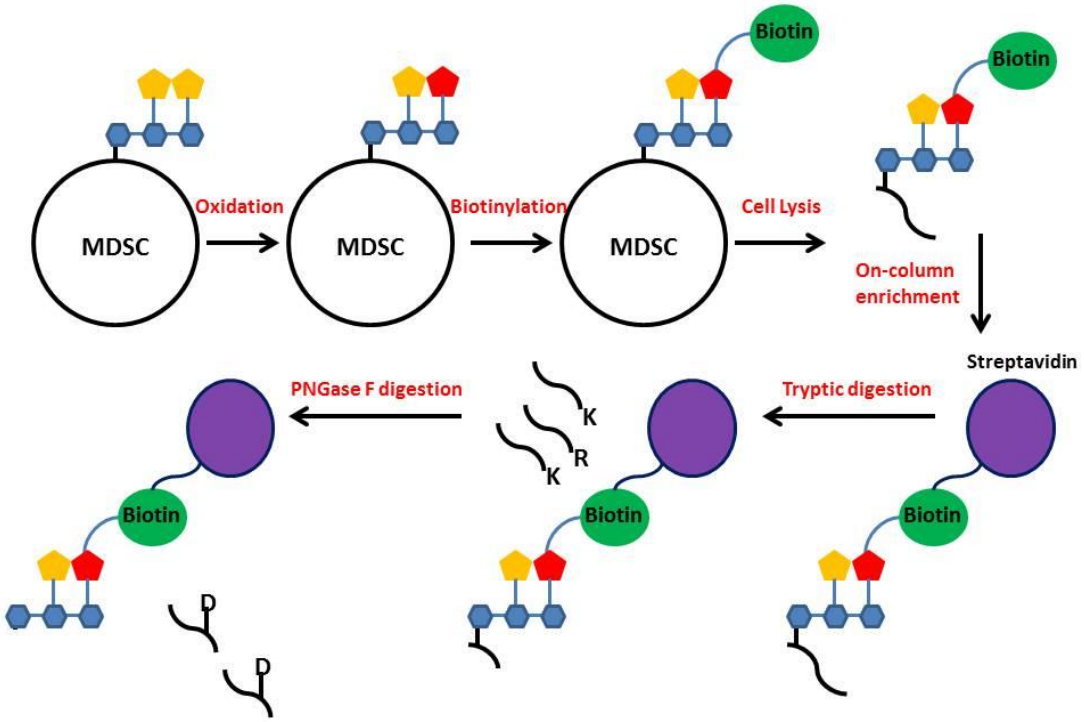

Figure 8. A schematic representation of the cell surface enrichment technique described in the methods section. It should be noted the oxidized glycan is indicated by the change in sugar moiety from yellow to red.

Analysis via mass spectrometry

As previously described for the analysis of the nanowire pellicle, both fractions were analyzed using the Shimadzu Prominent nanoHPLC in line with the LTQ-orbitrap XL. Due to a lack of knowledge of final peptide concentration, a test injection was performed for each sample type. Once the best signal intensity was established a maximal number of injections was made using the optimal injection volume. Each sample was trapped using a Zorbax 300SB-C18 column (0.3x5mm) using solvent A (97.5% water, 2.5% acetonitrile, 0.1% formic acid) at a flow rate of 10ul/minute. The analytical column utilized was once again the EVEREST C18 column. The samples were fractionated at a flow rate of 500nl/minute using a three hour linear gradient of

5% solvent B to 80% solvent B (97.5% acetonitrile, 2.5% water, 0.1% formic acid). Instrument parameters utilized during the pellicle experiment analysis were kept for the analysis of these samples.

Bioinformatics

As with the pellicle method, Thermo Xcalibur 2.0 was used to store all .RAW files (Thermo Fisher Scientific, CA). PepArML was once again used to make protein assignments to both fractions against the UniProtKnowledgebase (May 2012 version)[19]. For the tryptic fraction, search parameters mirrored those utilized for the pellicle samples: enzyme cleavage- tryptic, variable modifications- oxidation of methionine, fixed modifications- carbamidomethylation of cysteine. However, due to the nature of the cleavage used to liberate the glycopeptides special consideration was taken in the search parameters. These fractions were searched with the additional variable modification of deamidation. This modification occurs as a direct result of PNGase F cleavage of N-linked glycosylation and can act as an indicator of methodology success. Protein identifications yielded by the tryptic fraction were required to have two or more unique peptides, with an overall false discovery rate of 10% or less. Protein identifications yielded by the PNGase F fraction were based on only a single peptide. This exception was made to account for the possibility of only one N-linked glycosylation site on the protein, which would yield only one peptide liberated by PNGase F.

Results and Discussion

Evaluation of the viability of the enrichment technique

The use of the aminooxy-biotin enrichment technique was evaluated in several ways. The first, most macroscopic, was the assessment of the enrichment of cell surface proteins yielded by each fraction (Table 4). The category of "cell surface" included proteins that were

classified as plasma membrane, plasma membrane associated, apical membrane, external to the plasma membrane, cell edge, cell leading edge, and cell junction. As can be seen in Table 4, the cell surface enrichment reaches over 50% in both the tryptic and PNGase F digested fractions. Furthermore, in comparing these enrichment values we observe the PNGase F products to have higher surface enrichment. Included in Table 4 are the enrichment values for both cytoskeletal and extracellular proteins. These proteins are also located at or near the cell surface. Therefore, it can be stated that they are a logical additional subset of proteins that may be captured by our tagging method. Furthermore, they may have interesting communicative functions within the tumor microenvironment and are thus of interest to us. If they are included in our enrichment percentage the enrichment reaches 77% for the tryptic fraction and 81.5% for the PNGase F fraction. These values are very promising, especially when compared to other enrichment techniques utilized within our group.

Sample Type	Proteins Identified	Peptides Identified	Cell Surface Enrichment	Cytoskeleton	Extracellular
Tryptic IDs	148	301	51%	11.5%	14.5%
PNGase F IDs	52	68	61%	1.5%	19%

Table 4. Summary of identifications and enrichment values for the cumulative set of protein identifications made within the tryptic fraction and the PNGase F fraction.

Aside from looking at enrichment values for the cumulative set of protein identifications, a cross-replicate comparison can also be made to assess reproducibility. In analyzing the results of each of two tryptic fractions (Figure 9), we observe fairly similar findings in that the majority of the proteins yielded by each fraction are cell surface, cytoskeletal, or extracellular. In looking at our contaminating protein identifications it is interesting to note a strong presence of nuclear

proteins in both replicates. This is somewhat unexpected given the series of high-speed centrifugations utilized to remove nuclear debris. It is possible there are some non-specific binding events causing contamination even during the on-column enrichment. Furthermore, because the MDSC are a heterogeneous population of cells found within a disease state it is possible they may have proteins typically assigned to the nucleus en route to an uncommon destination and thus able to be captured by this tagging method. Interestingly, ribosomal proteins are at a low abundance within this dataset. This is a promising indication of the viability of the tagging method as typically basic ribosomal proteins are readily detected in positive ion mass spectrometry. Thus, their absence suggests this method is successful in isolating our target proteome.

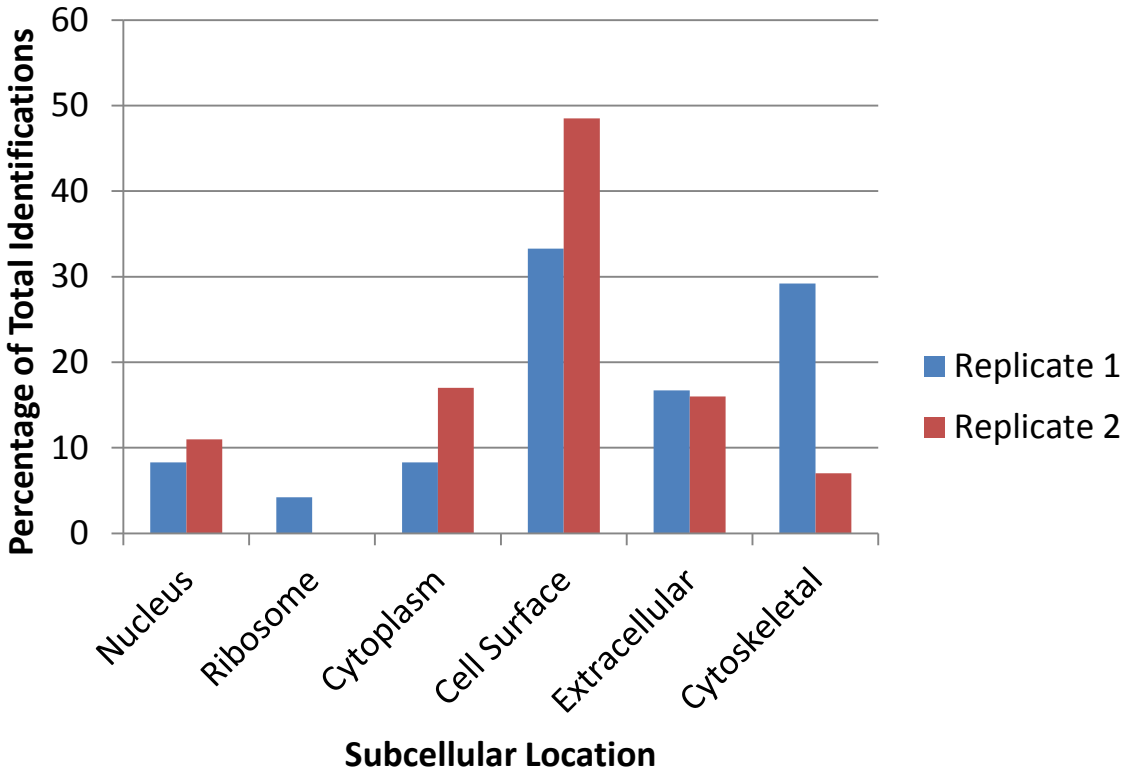

Figure 9. Subcellular location assignment of proteins identified from the tryptic fractions of two biological replicate experiments.

A comparison across three PNGase F fraction replicates, shown in Figure 10, suggests similar results to the tryptic fractions. Once again, the majority of proteins identified fall into the cell surface, cytoskeletal, or extracellular categories. In addition, the presence of nuclear and cytosolic proteins is very similar to the tryptic fraction. The presence of nuclear proteins is even more surprising within this fraction as the peptides yielded should strictly be those N-linked to tagged and captured glycans. The question of contamination via nonspecific binding is once again considered. However, the absence of ribosomal proteins in replicates 2 and 3 refutes this as they should also be contributing to contamination. Thus, it is possible these proteins are the result of a mis-assignment within the UniProtKnowledgeBase.

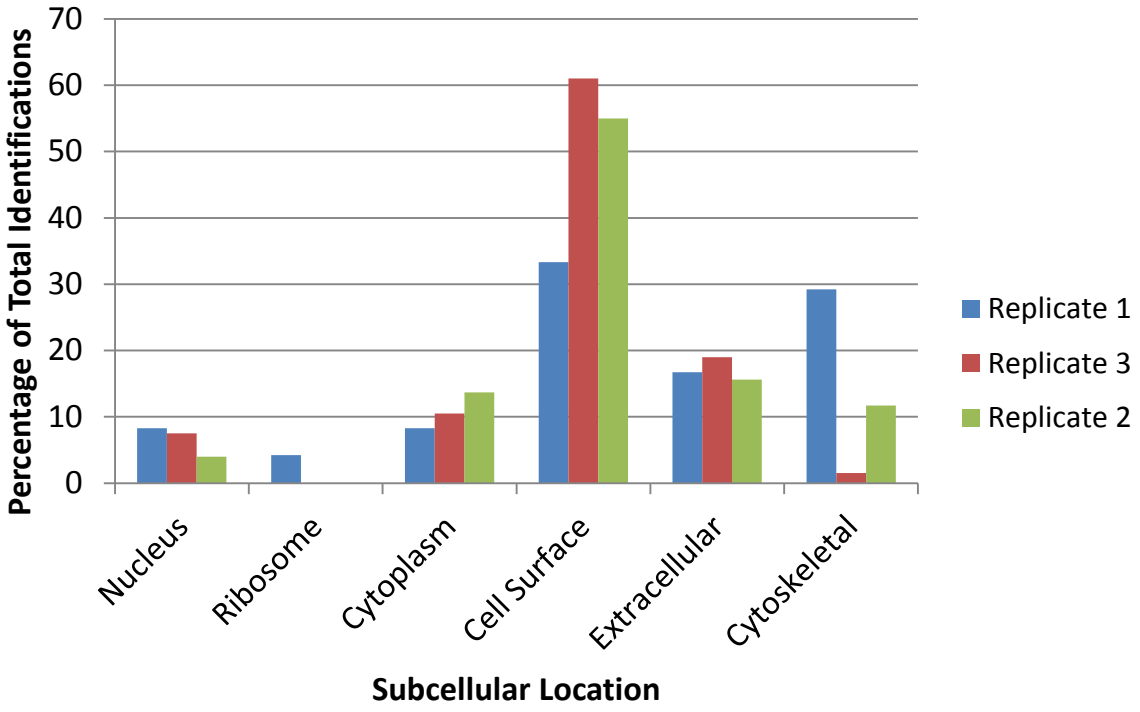

Figure 10. Subcellular location assignment of proteins identified from the PNGase F fractions of three biological replicate experiments.

Aside from subcellular location assignments, protein function assignments can also be made using the UniProtKnowledgeBase. Below (Figure 11) are the assignments for the cumulative list of proteins identified from both the tryptic and PNGase F fractions. While the

UniProtKnowledgeBase does not offer extremely specific categorizations, some basic conclusions can be drawn from the assignments made to the two fractions. As would be expected from a proteome isolated from the surface of cells, and thus likely to be involved in communication, the majority of the proteins have some type of binding activity. The vagueness of the protein binding and ion binding categories make it difficult to make specific statements regarding the types of protein-protein interactions occurring. There are also signal transducing and transporting proteins present in both fractions. Interestingly, there is a large set of nucleotide binding proteins. These may be contributed by those identifications assigned to the nucleus. However, it is interesting to suggest that perhaps there is some need for the shuttling of nucleotide binding proteins to the surface either for export or other communicative functions.

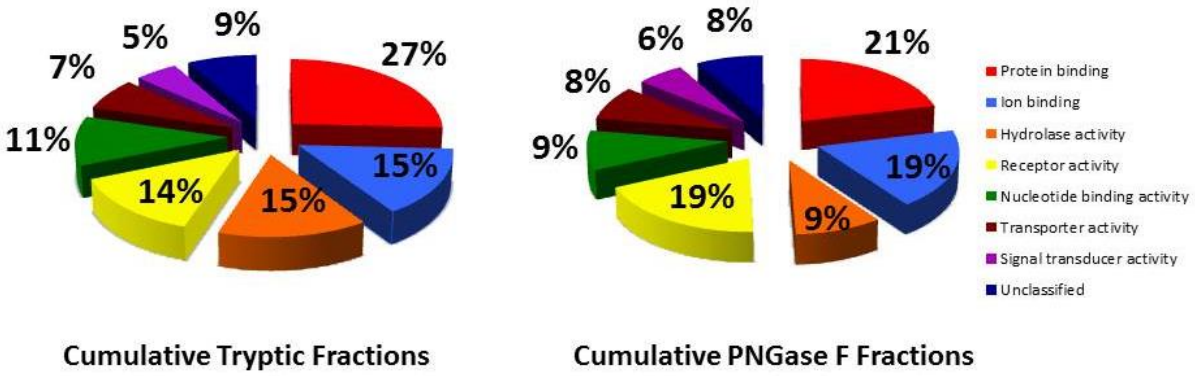

Figure 11. Subcellular functional assignment of the cumulative protein identifications yielded by each of the fractions. The tryptic fraction is based on a data set of 148 protein identifications, while the PNGase F is based on 52 identifications.

The presence of nuclear proteins, both within the subcellular location and function analyses, requires comment. As stated above, one explanation is the potential for mis-assignment of proteins within UniProt. It is possible that these proteins do indeed have a cell surface role that has not been established within the biological community to date. A second

explanation may be the use of nuclear proteins in specific, non-traditional, roles within the MDSC. While this has not been determined for this cell line, there are other examples available within the literature. One such example is that of the presentation of nuclear proteins at the surface under conditions of autoimmune disease. [34, 35, 36] Typically this presentation is associated with subsequent apoptosis, however the function of the nuclear protein presentation is still unclear. [34, 35, 36] The MDSC also exist within a disease state, and therefore it is plausible to suggest they have non-traditional surface proteins present.

While the assessment of the composition of protein identifications is useful, an assessment of the productivity of each replicate is also a worthwhile endeavor. A comparison of the overlapping identifications between each replicate offers insight as to the limitations of our tagging method (Figures 12 & 13). In comparing the identifications of replicates 1&2 yielded by the tryptic fractions we observe about half of each protein dataset is composed of unshared identifications. This suggests our tagging method, or the MS/MS identification, has not reached its capacity. The result is similar across the three PNGase F fractions (Figure 13). This phenomenon is further illustrated in Figure 14 in which the correlation between the three replicates and total number of protein identifications is explored for the PNGase F fractions. As the graph shows, there is a steady increase in protein identifications with each new experiment. Therefore it seems additional experiments would be useful in working to gain a better picture of the MDSC surface proteome.

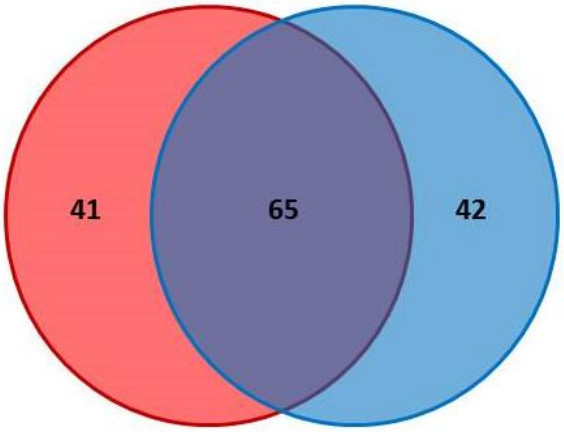

Figure 12. Assessment of the common protein identifications made between the tryptic fractions of replicates 1 (red) and 2 (blue).

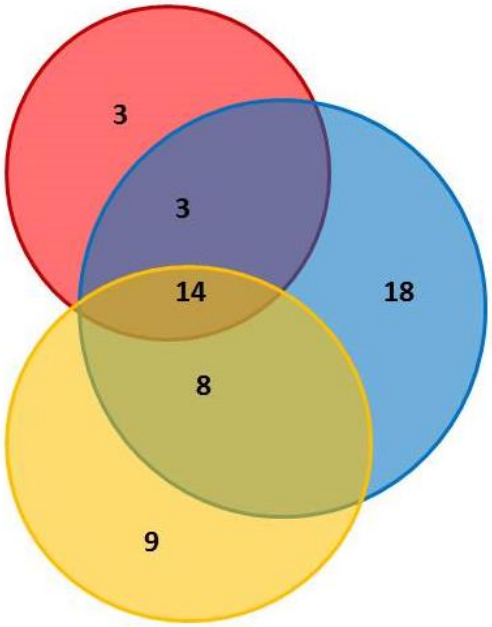

Figure 13. Assessment of the common protein identifications made between the PNGase F fractions of replicates 1 (red), 2 (yellow), and 3 (blue).

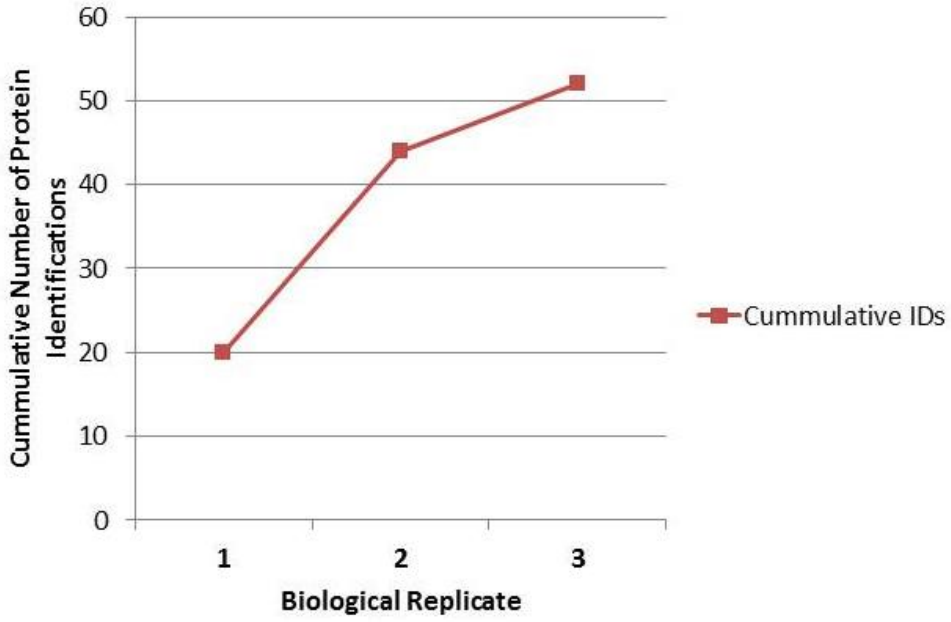

Figure 14. Correlation of cumulative number of protein identifications to additional biological experiments.

Assessment of the PNGase F fraction as an indicator of glycosylation

A further way to qualitatively assess the productivity of the labeling experiment is to analyze the presence of deamidation within the peptides yielded by the PNGase F fraction. The deamidation modification is an expected outcome of cleavage of a peptide from its N-linked glycosylation. Because our method is based upon glycan capture, it is expected that the vast majority of peptides found within the PNGase F fraction should contain this modification. However in looking for this modification only ten peptides, from 68 total peptides, (Table 5) were found to contain it. This is surprising as the method utilizes so many on-column washes prior to PNGase F digestion one would expect the majority of contaminants to have been removed, thus leaving only N-linked peptides present for enzymatic cleavage. The persistence of non-deamidated peptides suggests there is some amount of protein-protein interaction on-column, which results in the release of unmodified peptides within the PNGase F fraction.

Uniprot AC	Protein Name	Protein Description	Glycosylation Site
Q9D8U6	MCEM1_MOUSE	Mast cell-expressed membrane protein 1 homolog	AELSNVSDTVWNIR
Q61735	CD47_MOUSE	Leukocyte surface antigen CD47	DAMVGNYTCEVTELSR
Q61646	HPT_MOUSE	Haptoglobin	VVLHPNHSVVDIGLIK
Q2YFS1	PILB2_MOUSE	Paired immunoglobulin-like type 2 receptor beta-2	LILNWTQGQTSGVLR
P97797	SHPS1_MOUSE	Tyrosine-protein phosphatase non-receptor type substrate 1	GIANLSNFIR
P41245	MMP9_MOUSE	Matrix metalloproteinase-9	TSNLTDTQLAEAYLYR
P18572	BASI_MOUSE	Basigin	TQLTCSLNSSGVDIVGHR
P17809	GTR1_MOUSE	Solute carrier family 2, facilitated glucose transporter member 1	VIEEFYNQTWNHR
P11835	ITB2_MOUSE	Integrin beta-2	LNFTGPGEPDSLR
P08071	TRFL_MOUSE	Lactotransferrin	NSSNFHLNQLQGLR

Table 5. Proteins found to contain a deamidated N-X-S/T motif within the assigned peptides of the PNGase F fractions.

Further qualitative analysis of proteins of interest

In addition to studying the presence of glycosylation a manual assessment of the proteins identified was performed. One interesting subset of identifications was the cluster of differentiation, or CD, group of proteins. These proteins have been established as a specialized group of cell surface molecules involved in cell-to-cell communication, signaling, and adhesion. The terminology was originally developed as a way to classify antibodies found to identify these proteins on the surfaces of leukocytes. Currently, there are over 340 mouse CD protein categories and subcategories. Within this MDSC dataset 11 different CD proteins were identified (Table 6). Because of their role in cell communication they present naturally as a protein group of interest for further study both by our group and our collaborators. Within the 11 proteins found both CD14 and CD11b were identified. These proteins have been established as markers for MDSC and so their presence is not surprising, but rather a positive confirmation that

this method is capturing the MDSC surface proteome. While many CD proteins have been well characterized, an equal if not greater number are still poorly understood. Therefore, our list of 11 may offer interesting candidates for immunological study by our collaborators, which may lead to a greater understanding of the communication mechanisms enacted by the MDSC.

Cluster of Differentiation (CD) Proteins
CD14
CD98
CD43
CD37
CD47
CD177
CD97
CD11 antigen-like family member B
CD44 antigen precursor
CD121 antigen-like family member B
CD63 antigen

Table 6. A summation of the identified cluster of differentiation (CD) proteins found within either the tryptic or PNGase F fractions analyzed.

One CD found to be of particular interest is leukocyte surface antigen CD47. Not only is this protein glycosylated, it also was found to be present in all three biological replicates; LC-MS/MS analysis of the peptide used to identify this protein is shown below and offers strong indication that it is an acceptable identification (Figure 15). What makes it an identification of interest is not only its strength and pervasion of all three replicates, but its proposed biological roles. CD47 has been shown to play a role in mediating phagocytosis[26,27]. Namely, those cells found to have CD47 present on their surfaces are less likely to be engulfed by macrophages[26].

For a cell involved in immunosuppression, such as MDSC, this would be a valuable protein asset for defense against the body's natural immune defenses[26,27]. In addition to protecting the cell to which it is attached, CD47 has also been shown to interact with the glycoproteins on the surfaces of neighboring cells, such as T cells, to induce cell death[27]. These functions make CD47 a potential target for therapeutic work to hinder the immunosuppressive potency of MDSC.

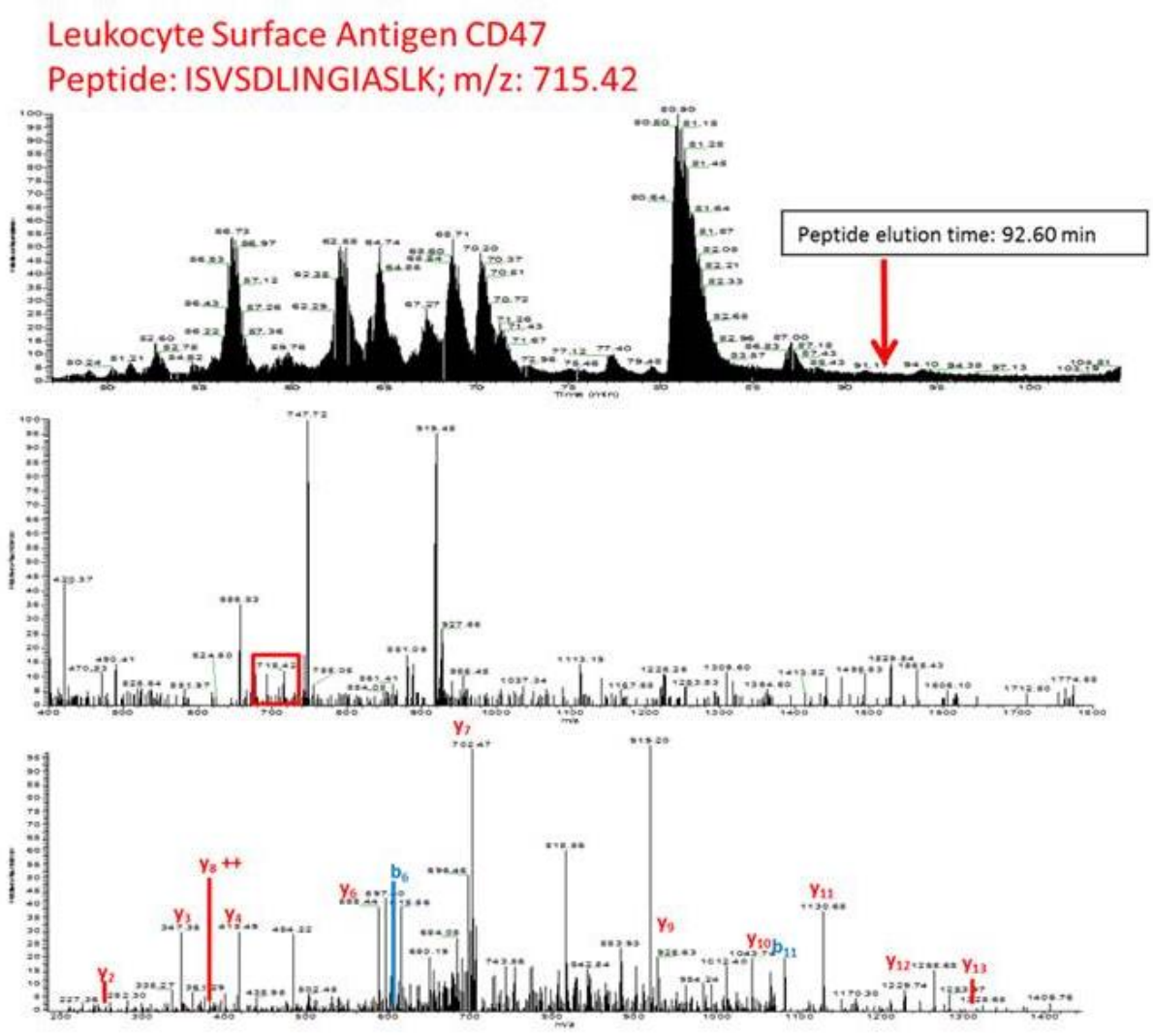

Figure 15. Identification of peptide ISVSDLINGIASLK from CD47. Top: total ion chromatogram, middle: precursor scan, bottom: fragmentation spectrum (MS2).

Another protein of particular interest in understanding the function of MDSC is the heterodimer S100A8/A9. Our collaborators at UMBC have established the chemotactic role of this protein within the tumor microenvironment[32]. They have shown the vital role it plays in recruiting increasing numbers of MDSC to the tumor site[32]. Within our study of the MDSC surface the protein S100A9 has been found in both the tryptic and PNGase F fraction. Its presence within the PNGase F fraction is very exciting as it would suggest the protein has some type of glycosylation present, and that its role in chemotaxis is enacted on the MDSC, as opposed to within the extracellular matrix. However, while it was identified in all three replicate experiments, no deamidation modification was found on the assigned peptides. Furthermore, an assessment of its sequence reveals it does not contain the classical N-X-S/T motif required for traditional N-linked glycosylation. However, it is possible there is O-linked glycosylation or even the presence of an as-of-yet unknown motif. Regardless of the glycosylation, its presence within the surface fractions is suggestive of surface based communication and MDSC recruitment within the tumor microenvironment.

Conclusions

Application of the oxidation/biotinylation cell surface glycan tagging was successful in isolating the MDSC surface proteome. Both the tryptic and PNGase F fractions yielded proteomic datasets that were enriched by a minimum of 35% over the MDSC whole cell lysate, excluding cytoskeletal and extracellular identification. Furthermore, the proteins identified are of interest to the communication pathways potentially being used by the MDSC to enact immunosuppression. Comparison of identifications across replicates revealed the surface of the MDSC is not saturated by the analysis and thus new identifications continue to be yielded by each replicate experiment. In taking a closer look at the identifications found, several proteins of

interest, such as the CD proteins, were identified as potential subjects of further study. To maximize our identifications, further analysis of the PNGase F fraction is needed to better understand the lack of deamidation and thus elucidate any potential adjustments needed to better maximize peptide yield.

Chapter 4: Conclusions

Both the cell surfaceome and plasma membrane proteome are current areas of special interest to the biochemical and biological community. The location of these proteins at the cell periphery makes them the most logical candidates for study in answering questions regarding cell-to-cell communication with a disease state. Many techniques have been developed to isolate the cell surface and plasma membrane from the remaining cellular parts. Previous nanoparticle pellicle techniques have yielded enrichments as high as 38%.[15] When observing other surface tagging systems we find lectin-affinity tags enrich approximately 40% for the cell surface, while in vitro use of a sulfo-NHS-LC-biotin tag has yielded 73% enrichment.[37, 38] In one experiment *in vivo* the same biotin strategy yielded 37% enrichment.[39]

Here we have utilized two different techniques to determine the best course of action for the isolation and study of the MDSC surface. While the nanowire pellicle method does show promise in the isolation of transmembrane proteins, our current implementation of this technique, utilizing nanowires, does not offer as successful an enrichment value as the biotin tagging technique, approximately 56% cell surface proteins. Therefore, in moving forward with the study of the MDSC, and other components of the tumor microenvironment, the latter technique should be applied. It should be noted that while the enrichment values yielded by this technique were promising, some optimization of on-column digestion conditions may be considered to increase yields of deamidated peptides following PNGase F digestion. These may include further washing with denaturing agents to better remove non-specifically bound proteins.

The nanowire pellicle method does show viable application in the isolation of transmembrane proteins of low abundance. Furthermore, this technique may be of particular interest to individuals not wishing to alter the surface glycoproteins via covalent tagging, as is

the case with biotinylation. If one chose the nanowire pellicle as their enrichment technique, further steps should be taken to optimize lysis for their target cell line. This optimization may aid in creating the best average pellicle size fragment distribution for separation and analysis.

Bibliography

1. Overington, J.P., Al-Lazikzni, B., Hopkins, A.L. How many drug targets are there? *Nature Reviews Drug Discovery*. **2006**. 5, 993-996.

2. Cordwell, S.J., Thingholm, T.E., Technologies for plasma membrane proteomics. *Proteomics*. **2010**. 10, 611-627.

3. Speers, A.E., Wu, C.C., Proteomics of integrals membrane proteins: theory and application. *Chemical Reviews*. **2007**. 107, 3687-3725.

4. Chaney, L.K., Jacobson, B.S. Coating cells with colloidal silica for high yield isolation of plasma membrane sheets and identification of transmembrane proteins. *Journal of Biological Chemistry*. **1983**. 258, 10062-10072.

5. Zhang, H., Li, X., Martin, D.B., Aebersold, R. Identification and quantification of N-linked glycoproteins using hydrazide chemistry, stable isotope labeling and mass spectrometry. (2003) *Nature Biotechnology.* **2003**. 21(6), 660-666.

6. Zeng, Y., Ramya, T.N.C., Dirksen, A., Dawson, P.E., and Paulson, J.C. High efficiency labeling of glycoproteins on living cells. *Nature Methods.* **2009**. 6(3), 207-209.

7. Nilsson, J., Ruetschi, U., Halim, A., Hesse, C., Carlsohn, E., Brinkmalm, G., and Larson, G. Enrichment of glycopeptides for glycan structure and attachment site identification. *Nature Methods.* **2009**. 6(11) 809-813.

8. Wollscheid, B., Bausch-Fluck, D., Henderson, C., O'Brien, R., Bibel, M., Schiess, R., Aebersold, R., and Watts, J.D. Mass-spectrometric identification and relative quantification of N-linked cell surface glycoproteins. *Nature Biotechnology*. **2009**. 27(4), 378-386.

9. Weekes, M.P., Antrobus, R., Lill, J.R., Duncan, L.M., Hor, S., and Lehner, P.J. Comparative analysis of techniques to purify plasma membrane proteins. *Journal of Biomolecular Techniques.* **2010**. 21, 108-115.

10. Ghosh, D., Korkhin, O., Antonovici, M., Eris, W., Standing, K.G. Beavis, R.C., Wilkins, J.A. Lecitn affinity as an approach to the proteomic analysis of membrane glycoproteins. *Journal of Proteome Research,* 2004, *3* (4), pp 841–850

11. Rahbar, A.M., Fenselau, C. Integration of Jacobson's pellicle method into proteomic strategies for plasma membrane proteins. *Journal of Proteome Research*. **2004**. 3, 1267-1277.

12. Prior, M.J., Larance, M., Lawrence, R.T. Qualitative proteomic analysis of the adipocyte plasma membrane. *Journal of Proteome Research*. **2011**. 10, 4970-4982.

13. Li, X., Jia, X., Xie, C. Development of cationic colloidal silica-coated magnetic nanospheres for highly selective and rapid enrichment of plasma membrane fractions for proteomic analysis> *Biotechnology Applications in Biochemistry*. **2009**. 54, 213-220.

14. Li, X., Jin, Q.,m Cao, J. Evaluation of two cell surface modification methods for proteomic analysis of plasma membrane from isolated mouse hepatocytes. *Biochimica Biophysica Acta*. **2009**. 1794, 32-41.

15. Choksawangkarn, W., Kim, S.K., Cannon, J.R., Edwards, N.J., Lee, S.B., Fenselau, C. Enrichment of plasma membrane proteins using nanoparticle pellicles: comparison between silica and higher density nanoparticles. *Journal of Proteome Research*. **2013.** 12, 1134-1141.

16. Zhang, W., Zhao, C., Wang, S. Coating cells with cationic silica-magnetite nanocomposites for rapid purification of integral plasma membrane proteins. *Proteomics*. **2011**. 11, 3482-3490.

17. Kim, S.K., Choksawankarn, W., Rose, R., Fenselau, C., Lee, S.B. Nanowire pellicles for eukaryotic cells: nanowire coating and interaction with cells. *Nanomedicine*. **2014**. 9(8), 1171-1180.

18. Kim, S.K., Rose, R., Choksawangkarn, W., Graham, L., Hu, J., Fenselau, C., Lee, S.B. Comparison of nanowire pellicles for plasma membrane enrichment: coating nanowires on cell. *Journal of Nanoparticle Research.* **2014**. 15(12), 2133-2141.

19. Edwards, N., Wu, X., Tseng, C. W. An unsupervised, modelfree, machine-learning combiner for peptide identifications from tandem mass spectra. *Clinical Proteomics.* **2009**. 5,23-36.

20. Gabrilovich, D. I., and Nagaraj, S. Myeloid-derived suppressor cells as regulators of the immune system. *Nature Reviews: Immunology.* **2009.** 9, 162-174.

21. Kusmartsev, S., and Gabrilovich. D.I. Role of immature myeloid cells in mechanisms of immune evasion in cancer. *Cancer Immunology and Immunotherapy.* **2006**. 55, 237-245.

22. Chornoguz, O., Grmai, L., Sinha, P., Artemenko, K.A., Zubarev, R.A., and Ostrand-Rosenberg, S. Proteomic pathway analysis reveals inflammation increases myeloid-derived suppressor cell resistance to apoptosis. *Molecular and Cellular Proteomics.* **2011**. 10(3), 1-9.

23. Bunt, S.K., Sinha, P., Clements, V.K., Leips, J., and Ostrand-Rosenberg, S. Reduced inflammation in the tumor microenvironment delays the accumulation of myeloid-derived suppressor cells and limits tumor progression. *Journal of Immunology.* **2005**. 176, 284-290.

24. Ostrand-Rosenberg, S., and Sinha, P. Myeloid-derived suppressor cells: linking inflammation and cancer. *Journal of Immunology.* **2009**. 182, 4499-4506.

25. Hanson, E.M., Clements, V.K., Sinha, P., Ilkovitch, D., Ostrand-Rosenberg, S. Myeloid-derived suppressor cells down-regulate L-Selectin expression on CD4+ and CD8+ T cells. *Journal of Immunology.* **2009**. 183, 937-944.

26. Oldenborg, P.A. CD47: A cell surface glycoprotein which regulates multiple functions of hematopoietic cells in health and disease. *Hematology*. **2013**, 1-19.

27. Olsson, M., Nilsson, A., Oldenborg, P.A. Target cell CD47 regulates macrophage activation and erythrophagocytosis. *Transfusion Clinique et Biologique***. 2006.** 13, 39-43.

28. Sinha, P., Okoro, C., Foell, D., Freeze, H.H., Ostrand-Rosenberg, S., Srikrishna, G. Proinflammatory S100 proteins regulate the accumulation of myeloid-derived suppressor cells. *The Journal of Immunology*. **2013**. 181, 4666-4675.

29. Gebhardt, C., Nemeth, J., Angel, P., Hess, J. S100A8 and S100A9 in inflammation and cancer. *Biochemical Pharmacology*. **2006**. 72, 1622-1631.

30. Ghavami, S., Chitayat, S., Hashemi, M., Eshraghi, M., Chazin, W., Halayko, A., Kerkhoff, C. S100A8/A9: A janus-faced molecule in cancer therapy and tumorgenesis. European *Journal of Pharmacology*. **2009**. 625, 73-83.

31. Lackmann, M., Rajasekariah, P., Iismaa, S.E., Jones, G., Cornish, C.J., Hu, S., Simpson, R.J., Moritz, R.L., Geczy, C.L. Identification of a chemotactic domain of the pro-inflammatory S100 protein CP-10. *Journal of Immunology*. **1993**. 150, 2981-2990.

32. Burke, M., Choksawangkarn, W., Edwards, N.J., Ostrand-Rosenberg, S., Fenselau, C. Exosomes from myeloid-derived suppressor cells carry biologically active proteins. *Journal of Proteome Research.* **2014**. 13(2), 836-843.

33. Krogh, A., Larsson, B., von Heijne, G., Sonnhammer, E.L.L.. Predicting transmembrane protein topology with a hidden Markov model: Application to complete genomes. *Journal of Molecular Biology*.**2001**. 305(3), 567–580.

34. Jordan, P., Kubler, D. Autoimmune diseases: nuclear autoantigens can be found at the cell surface. *Molecular Biology Reports*. **1996**. 22(1), 63-66.

35. Dieker, J., Muller, S. Post-translational moditifactions, subcellular relocation and release in apoptotic microparticles: apoptosis turns nuclear proteins into autoantigens. *Folia Histochemica et Cytobiologica*. 2009. 47(3), 343-348.

36. McArthur, C., Wang, Y., Veno, P., Zhang, J., Fiorella, R. Intracellular trafficking and surface expression of SS-A (Ro), SS-B (la), poly(ADP-ribose) polymerase and alpha-fodrin autoantigens during apoptosis in human salivary gland cells induced by tumour necrosis factor-alpha. *Archives of Oral Biology*. **2002.** 47(6), 443-448.

37. Ghosh, D., Krokhin, O., Antonovici, M., Ens, W., Standing, K.G., Beavis, R.C., Wilkins, J.A. Lectin affinity as an approach to the proteomic analysis of membrane glycoproteins. *Journal of Proteome Research*. **2004**. 3(4), 841-850.

38. Nunomura, K., Nagano, K., Itagaki, C., Taoka, M., Okamura, N., Yamauchi, Y., Sugano, S., Takahashi, N., Izumi, T., Isobe, T. Cell surface labeling and mass spectrometry reveal diversity of cell surface markers and signaling molecules expressed in undifferentiated mouse embryonic stem cells. *Molecular and Cellular Proteomics*. **2005.** 4(12), 1968-1976.

39. Rybak, J.N., Ettorre, A., Kaissling, B., Giavazzi, R., Neri, D., Elia, G. In vivo protein biotinylation for identification of organ-specific antigens accessible from the vasculature. *Nature Methods*. **2005**. 2(4), 291-298.